Characterisation of mechanically alloyed Ti–Al–B nanocomposite consolidated by spark plasma sintering

H. B. Lee, S. H. Kim, S. W. Kang and Y. H. Han

The microstructure and mechanical properties of TiB_2/Al nanocomposites based on the Ti–Al–B system, consolidated by spark plasma sintering of mechanically alloyed activated nanopowders, have been characterised. Mechanical alloying was carried out in a planetary ball mill for 120–180 min at 350 rev min^{-1}. The powders were pressed in vacuum at a pressure of 60 MPa; a dc current of 1800 A was applied for 4 min, generating a maximum temperature in the graphite mould of 1400°C. Analysis of the synthesised nanocomposites by SEM, XRD, and TEM showed them to consist of TiB_2 second phase particles, 10–30 nm in size, in a near amorphous Al phase, with unreacted Ti and B on grain boundaries as a ternary phase. Composites consolidated from powders mechanically alloyed from an initial elemental powder mix of 0·3 mol Al, 0·7 mol Ti, and 2·0 mol B achieved the best relative density (98%) and bending strength (847 MPa); the highest Vickers hardness of 19·6 GPa was achieved for the 0·1:0·9:2·0 mol starting composition. BCT/608

Dr Lee, Dr Kim, and Dr Kang are in the Department of Inorganic Materials Engineering, Myong-Ji University, Yongin 449–728, Republic of Korea. Dr Han is in the Department of Chemical Engineering and Materials Science, University of California, Davis, CA 95616, USA (yhhan@ucdavis.edu). *Manuscript received 19 May 2003; accepted 29 September 2003.*

INTRODUCTION

Industry increasingly requires advanced properties in refractory composite materials, for example improved hardness, purity, and chemical stability, and more economical processing. Carbide, boride, and nitride composites are of interest because of their superior mechanical properties and chemical stability relative to metals.[1,2] There is particular interest in TiB_2 ceramics because of their intermediate metal/ceramic character, with high melting point, remarkable hardness, good chemical stability, and high electrical conductivity. Thus, TiB_2 is expected to find application as a high temperature material, for high speed cutting tools, surface protection, armour cladding materials, refractories for Al smelting, electrodes for magnetohydrodynamicgenerators, and as an antiabrasive in corrosive environments.[3,4] Despite their excellent structural and electrical properties, TiB_2 ceramics are known to be very difficult to consolidate because of their strong covalence (and hence limited ductility) and thermal expansion anisotropy.[5] Conventional consolidation involves heating elemental powders or mixtures to close to their melting point, consuming excessive energy but achieving almost full densification.

Recently much research has focused on adding metals or ceramics to TiB_2 to improve its mechanical properties by suppressing grain growth, as well as on a new technique being developed for consolidation of TiB_2.[6–8] A route involving mechanical alloying followed by SPS (spark plasma sintering) is well suited for this purpose. The mechanical alloying step involves high energy ball milling of elemental powders to produce a 'synthesised' powder that is very different in character and microstructure. SPS provides rapid consolidation with greatly reduced heat input.

Mechanical alloying is widely used for nanomaterial processing. The principle of the technique is that powders are continually welded and fractured by the action of the balls to produce a homogeneous, finely dispersed, alloyed solid phase at close to room temperature without the presence of liquid phase; composites prepared from these powders have superior compositional properties to those prepared by rapid cooling or metal matrix composite phase hardening.[9–11]

The SPS technique produces rapid consolidation of ceramic powders to high densities, by generating an electron plasma in the particle compact. The surfaces of the particles become activated and self-heating is generated among particles, producing thermal change and mass change in a very short time.[12–15] Thus, rapid densification is achieved through a microscale heating processes.

Mechanically alloyed powders allow lower processing temperatures owing to their higher surface activation and stored energy; consolidation is achieved more rapidly, and higher density and finer microstructure may also be obtained. In the present study, the microstructure and mechanical properties of Ti–Al–B nanocomposites consolidated from mechanically alloyed composite powders have been characterised.

EXPERIMENTAL PROCEDURES

Mechanical alloying

Starting elemental powders used were Ti (Osaka Titanium Co., 99·0% purity, −325 mesh), B (Aldrich Chemical Co., 95% purity, −325 mesh), and Al (Aldrich Chemical Co., 99% purity, −200 mesh). Three initial compositions were mechanically alloyed, consisting of Ti/Al/B elemental molar ratios of 0·9:0·1:2·0, 0·7:0·3:2·0, and 0·5:0·5:2·0. Mechanical alloying was performed in a planetary ball mill with a ball/powder ratio of 10:1 at 350 rev min^{-1}. Milling in vacuum was continued until no further reaction was observed (typically for 150–180 min). Samples were checked by X-ray diffractometry (XRD) every 30 min to determine the progress of synthesis.

Consolidation of nanocomposites by SPS

The powder obtained just before synthesis was complete was chosen for consolidation as being in the optimum state to minimise grain growth and allow full densification at low sintering temperature. As shown in the overview of

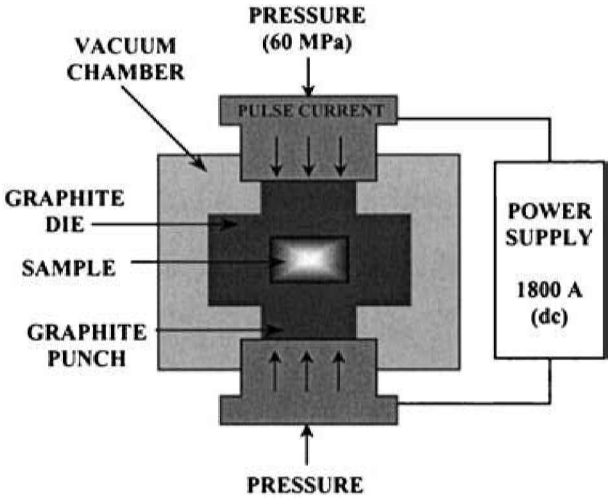

1 Overview and schematic diagram of SPS process

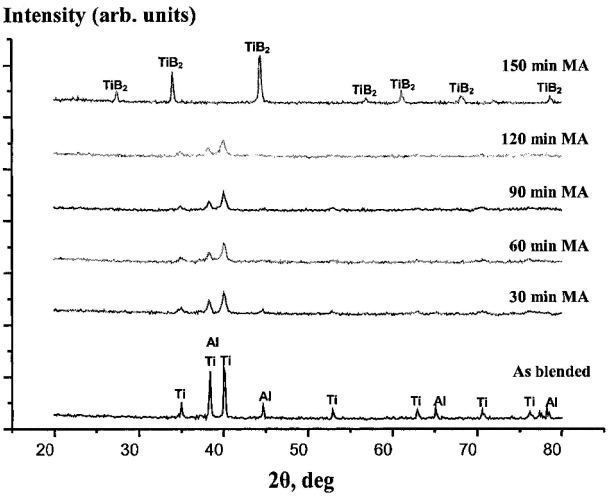

3 XRD patterns of mechanically alloyed 0·3 mol Al composition as function of milling time

SPS in Fig. 1, the mixture was loaded and pressed under 60 MPa in vacuum, and an 1800 A dc electric current was applied until a temperature of 1400°C was reached on the surface of the graphite mould. This took about 4 min, after which the power was switched off and the chamber allowed to cool.

Microstructural analysis and mechanical property measurement

Synthesised powders and the phases in the sintered body were analysed by XRD (Shimadzu model XD-DI, Cu K_α). Microstructure and particle size in the compositions were observed by SEM (Philips 515) and TEM (Joel JEM-3011), and quantitative phase analysis was conducted using EDS (Leica Cambridge Ltd, Oxford). The density of sintered bodies was determined according to Korean standard KSL 3114 for porosity, absorption, and specific gravity measurement in refractory bricks. The sintered specimen was boiled at 100°C for 3 h to calculate the volume from the weight of buoyancy and bubbles for dried weight. To obtain the relative density of the composite, specific weight was divided by theoretical density.

An Instron mechanical tester (Instron Japan, model 4204) was used at 0·5 mm min^{-1} cross-head speed, with 15 mm span distance for three point bending strength applying a fracture load. For hardness measurement, a Vickers indenter was applied on the polished surface under a load of 10 kgf for 10 s at 50 μm s^{-1}.

RESULTS AND DISCUSSION

Characteristics of synthesised powder

The effects of mechanical alloying have been well explained in terms of high energy impacts causing severe plastic deformation, fracture, and cold welding of powder. Owing to the small scale of the microstructure and enhanced diffusivity of species, solid state reactions and/or phase transformations can occur in powders during milling or at much lower temperatures during subsequent heating in SPS consolidation.

As expected, the initial powder composition critically affected consolidation and mechanical properties. XRD scans for three initial powder mixes as mechanical alloying proceeds are shown in Figs. 2–4. The peaks tend to become weaker but broader with time, a common phenomenon in mechanical alloying that results from the internal stress and high densities of lattice defects in the powder and leads to microstructural refinement and powder homogenisation, and in some instances to amorphisation of the strucutre.[10]

Increasing milling time up to 120–180 min produced a sudden change of phase, with the appearance of new peaks representative of TiB_2 and the disappearance of peaks of Ti and Al. At room temperature, synthesis appears to occur

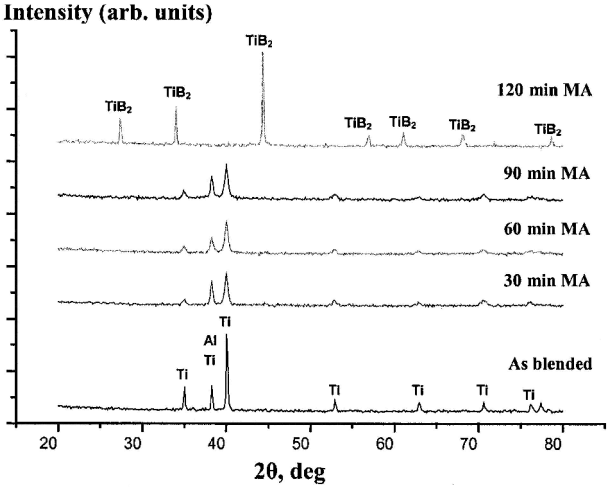

2 XRD patterns of mechanically alloyed 0·1 mol Al composition as function of milling time

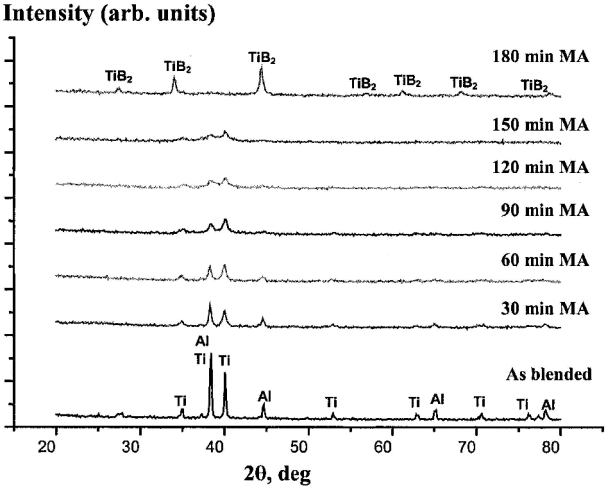

4 XRD patterns of mechanically alloyed 0·5 mol Al composition as function of milling time

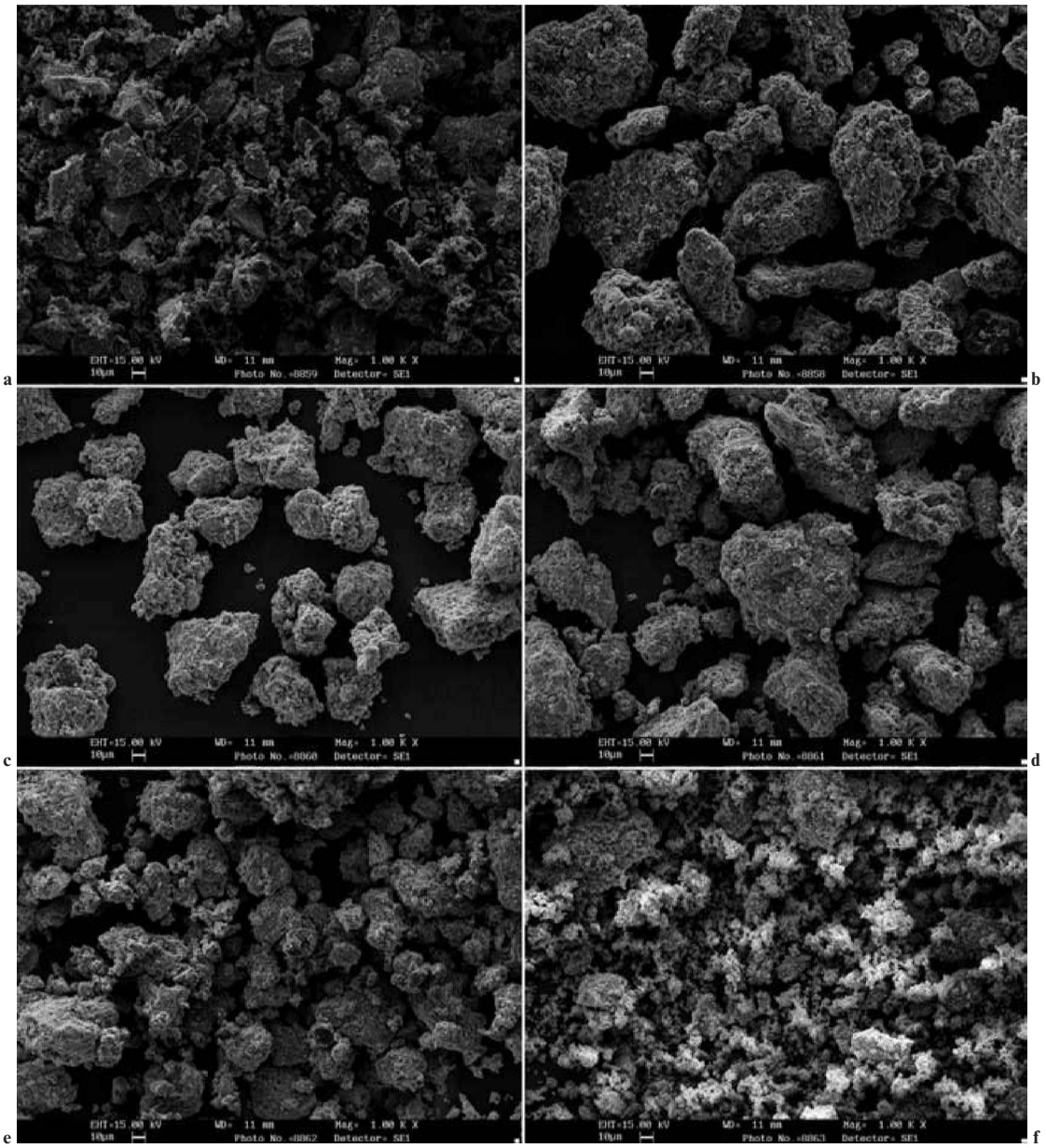

5 SEM micrographs of mechanically alloyed 0·3 mol Al composition as function of milling time: *a* as blended, *b* 30 min, *c* 60 min, *d* 90 min, *e* 120 min, *f* 150 min

during milling with no introduction of direct or indirect thermal energy, as reported by Tokita.[12,15] The generation of a more homogenised powder with a higher specific surface area by grinding the powder mixture to a smaller size before mechanical alloying would be beneficial in producing higher activation, leading to a lowering of synthesis temperature.[16]

Change of microstructure with mechanical alloying time in the 0·3 mol Al composition is shown in Fig. 5. Figure 5*a* is before mechanical alloying of the mixture, and Fig. 5*b* with some flake phase observed after 30 min. Initially, flake shaped particles appear to form as a result of powder particles being compressed between ball and ball or ball and wall. As milling time increases, particles gradually become more spherical, and individual particles become increasingly layered as a result of contact between fine micropowders. The change in macroparticle size, layered with microfine powder, with time is caused by a continuous contact pressure and fracture mechanism.

Figure 5*e* is just before the complete synthesis stage (mechanical alloying for 120 min) and Fig. 5*f* just after

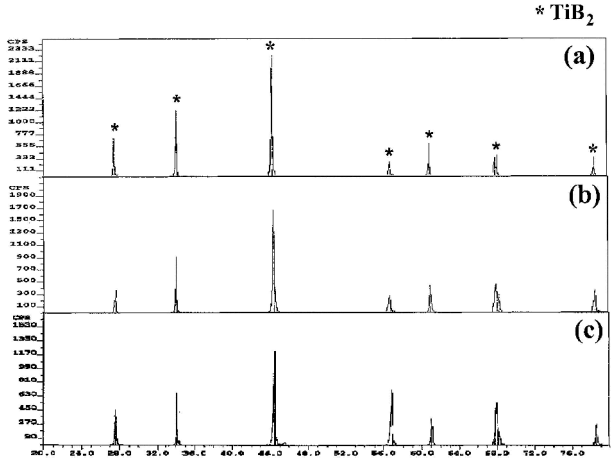

6 X-ray diffraction patterns of Ti–Al–B composites sintered by SPS: *a* composition 0·1, *b* composition 0·3, *c* composition 0·5

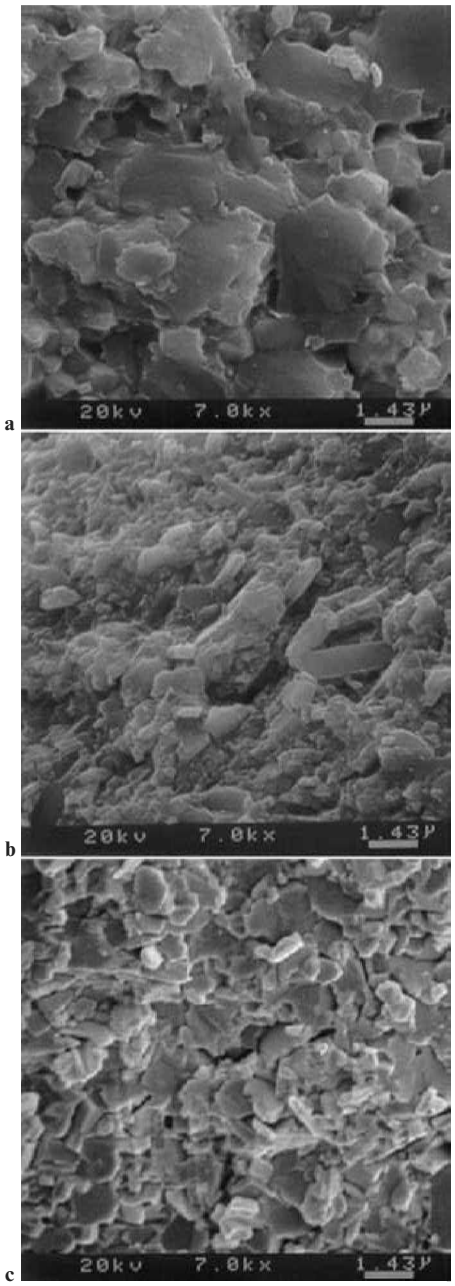

7 SEM micrographs of Ti–Al–B composites sintered by SPS: *a* composition 0·1, *b* composition 0·3, *c* composition 0·5

complete synthesis at 150 min. The particle (as opposed to agglomerate) size after synthesis is very fine (< 300 nm), as shown in Figure 5*f*; submicrometre size is also observed just before the synthesis stage in Fig. 5*e*. This proves that the submicrometre size mixture could be obtained just before the synthesis stage by mechanical alloying.

Characteristics of sintered body

The XRD pattern of the sintered body consolidated by SPS shows TiB_2 peaks only, as shown in Fig. 6. No Al peaks are detected, although the higher Al composites have lower TiB_2 peak intensity. Residual Al on TiB_2 grain boundaries seems to remain in an amorphous state during rapid cooling after SPS.

Fracture surfaces of Ti–Al–B composites are shown in Fig. 7. In general, with increasing Al content, the presence of a greater quantity of liquid phase would be expected to separate the boride particles, leading to a morphology more typical of interfacial fracture.

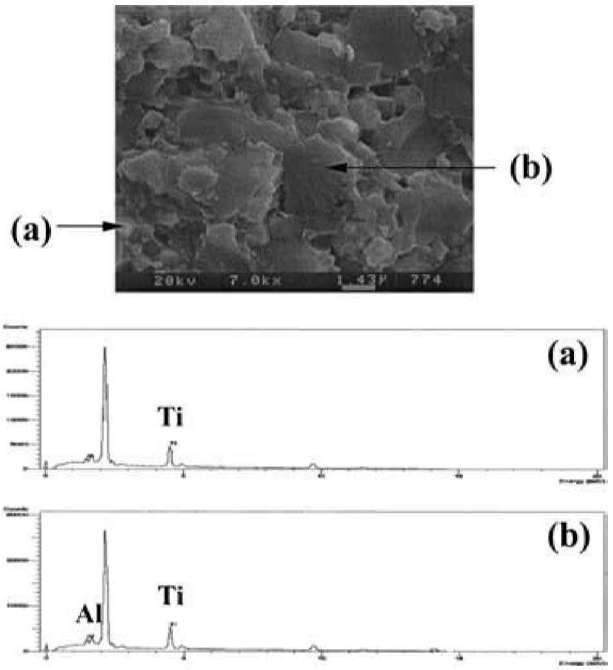

8 EDS results for composition 0·1 sintered by SPS

Figure 7*a* (0·1 mol Al) shows the largest particle size of the three compositions, but seems denser, with an irregular distribution of Al over the fracture surface. Figure 7*b* (0·3 mol Al) shows smaller particle size, indicating the smallest particle of Al on the fracture surface that could act as a fracture initiating defect. In Fig. 7*c* (0·5 mol Al), precipitated Al exists on the TiB_2 particle faces, presumably as a result of the presence of a liquid phase during sintering, which is considered to lead to cracking during rapid cooling following SPS.

Compositional analysis was performed by EDS on interesting microstructures detected in the SEM micrographs, as shown in Figs. 8–10. In Fig. 8 (0·1 mol Al), only Ti was detected in fine particles (a), whereas 7·07 wt-%Al was detected in the larger particle (b). In Fig. 9 (0·3 mol Al), the fine particles at (a) are considered to be TiB_2 phase; the larger particles at (b) and (c) consisted mostly of Ti with a little Al, having compositions very close to that of particle (b) in Fig. 8. In Fig. 10 (0·5 mol Al), all particles, small or large, contained Ti and Al with a higher content (30–40 wt-%) of Al. No Al loss during consolidation in vacuum at 1400°C could be detected. No deposition of Al on the mould wall and no change in composition owing to evaporation were observed. It is considered that diffusion out of the boride network cannot occur to any significant extent in the time periods under consideration.

While XRD of the sintered body did not reveal the presence of Al, EDS showed contents of 7–40 wt-%Al, suggesting that Al is present in an amorphous state on the TiB_2 grain boundaries. The microfine, highly activated powders used in the present research, processed by mechanical alloying and SPS with low sintering temperature and time, appear to have suppressed grain growth. Thus, the large particles observed in the microstructure appear to be nanosize TiB_2 with an amorphous Al second phase present at grain boundaries.

Transmission electron microscopy was performed on film specimens from the bulk body, which was machined and ion milled by a Gatan PIPS ion miller. Figure 11 shows a TEM micrograph of a Ti–Al–B composite of about 500 nm particle size, in which numerous grain boundaries surrounding particles exist. EDS analysis (Fig. 12) showed particle

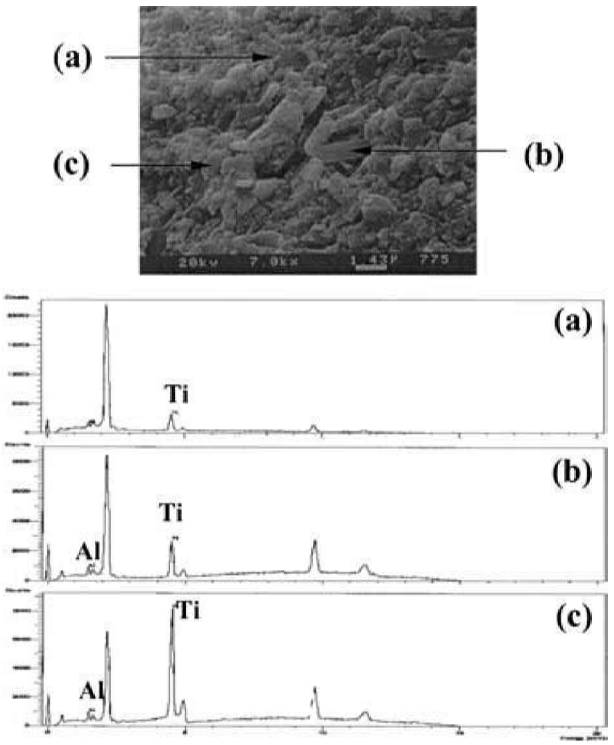

9 EDS results for composition 0·3 sintered by SPS

(a) to be crystalline with 10–30 nm grain size and to contain 97·48 wt-%Ti (considered to be TiB_2). The near spherical mechanically alloyed crystalline powder appears to prevent grain growth at short sintering times. The bright area (b) contains 86·64 wt-%Al plus unreacted Ti and B, and is likely to be a ternary amorphous phase, on the basis of an analysis by controlled sight diffraction pattern and EDS.

Figure 13 shows the relative density of Ti–Al–B nanocomposite consolidated by SPS. As noted from the SEM micrographs, the 0·3 composition considered the densest

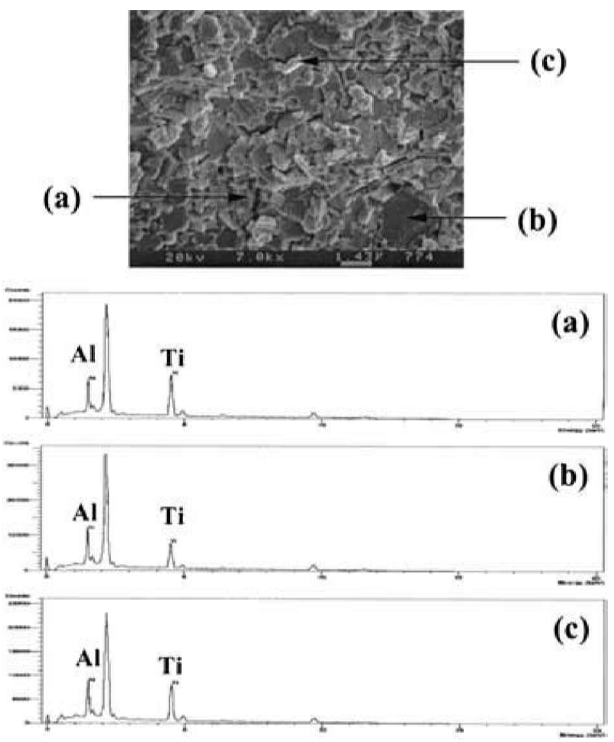

10 EDS results for composition 0·5 sintered by SPS

11 TEM micrograph of Ti–Al–B composite sintered by SPS

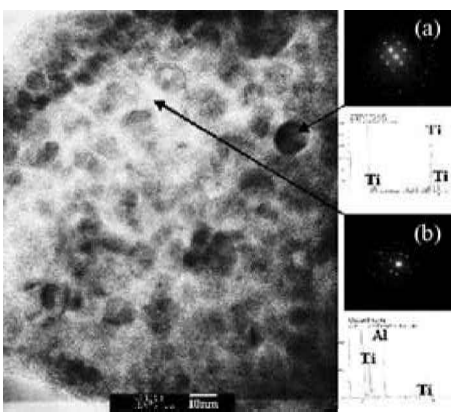

12 EDS analysis of Ti–Al–B composite sintered by SPS

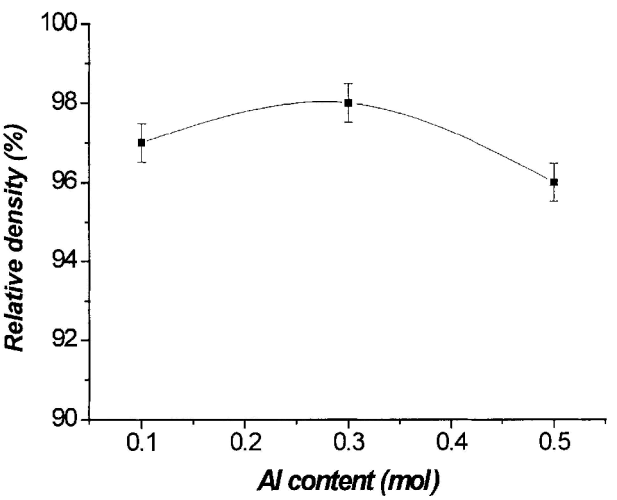

13 Relative density of Ti–Al–B composites sintered by SPS

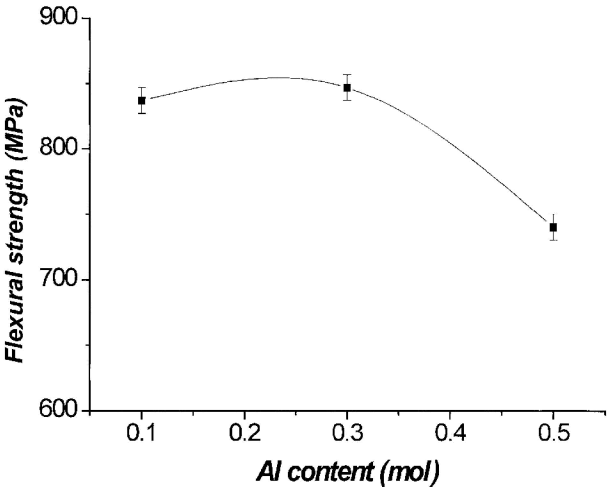

14 Flexural strength of Ti–Al–B composites sintered by SPS

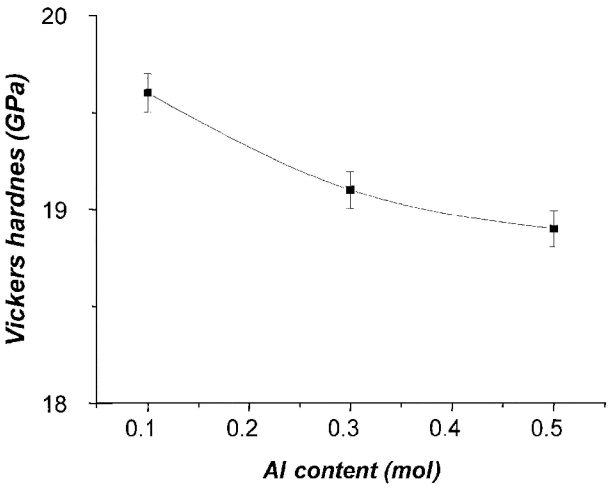

15 Vickers hardness of Ti–Al–B composites sintered by SPS

has a high value of 98%, and in the 0·5 mol Al composition with low relative density, liquid phase formation becomes more active with increasing Al addition, inducing cracking inside phases during rapid cooling in a short sintering time. Addition of Al enhances densification to some extent, but overdose of Al prevents densification with internal cracking.

Figure 14 shows the bending strength of the compositions of Al in the composite. All three compositions have very high strength values of 740–840 MPa, the highest (846·9 MPa) being the 0·3 mol Al composition. This excellent strength in the Ti–Al–B system can be explained in terms of full densification by liquid phase sintering with Al addition and prevention of grain growth staying at the nanosize level and of increasing relative crack length in fracture.

Figure 15 shows Vickers hardness measurements for the Ti–Al–B composites. Hardness decreased with increasing Al content, showing the highest value of 19·6 GPa in the 0·1 mol Al composition.

CONCLUSIONS

Activated nanopowders produced by mechanical alloying have been processed by SPS at 1400°C under 60 MPa pressure to produce Ti–Al–B nanocomposites. This work has led to the following conclusions.

1. It was confirmed by XRD and SEM studies that submicrometre size TiB_2 particles were obtained by mechanical alloying.

2. High density Ti–Al–B composites were successfully consolidated by SPS from the activated nanopowders obtained by mechanical alloying to just before complete reaction. These materials consist of TiB_2 crystalline particles of grain size 10–30 nm with an amorphous phase consisting of Al plus unreacted Ti and B at the grain boundaries.

3. The 0·3 mol Al composition (initial mix 0·7 mol Ti, 0·3 mol Al, 2·0 mol B) had the highest relative density (98% of theoretical) and bend strength (846·9 MPa). The 0·1 mol Al composition (0·9 mol Ti, 0·1 mol Al, 2·0 mol B) showed the highest hardness (19·6 GPa).

REFERENCES

1. F. W. VAHLDIEK: *J. Less-Common Met.*, 1967, **12**, 202–209.
2. K. E. SPEAR, P. MCDOWELL and P. MCMAHON: *J. Am. Ceram. Soc.*, 1986, **69**, c4.
3. A. D. MCLEOD, J. S. HAGGERTY and D. R. SADOWAY: *J. Am. Ceram. Soc.*, 1984, **67**, 705.
4. M. L. WILKINS: in 'Boron and refractory borides', (ed. Y. L. Matkovich), 633–648; 1977, New York, NY, Springer.
5. E. S. KANG, D. I. CHUNGAND and Y. K. PAEK: Proc. Ceramic Armor Materials Conf., 1990, 25–44.
6. J. A. KUSZYK and R. C. BRADT: *J. Am. Ceram. Soc.*, 1973, **56**, 420.
7. C. F. YEN, C. S. YUST and G. W. CLARK: in 'New developments and applications in composites', 317–330; 1979, Warrendale, PA, AIME.
8. R. Z. YUAN, Z. Y. FU, Z. A. MUNIR, X. X. ZHOU and Z. L. YANG: *J. Mater. Synth. Process.*, 1993, **1**, 153–157.
9. T. H. COURTNEY and D. MAURICE: *Scr. Mater.*, 1996, **34**, 5–11.
10. F. H. FROES, K. RUSSELL, C.-G. LIC, F. H. S. FROES and C. SURYANARAYANA: *Mater. Sci. Eng. A*, 1995, **192/193**, 612–623.
11. P. P. CHATTOPADHYAY, I. MANNA, S. TALAPATRA and S. K. PABI: *Mater. Chem. Phys.*, 1996, **68**, 85–94.
12. M. TOKITA: Proc. 2nd Symp. on SPS, 1997, 1.
13. M. TOKITA: Proc. 5th Int. Symp. on FGM, 1998, 71–76.
14. N. TAMARI, T. TANAKA, K. TANAKA and M. TOKITA: *J. Ceram. Soc. Jpn*, 1995, **103**, 740–742.
15. M. TOKITA: *J. Soc. Powder Technol. Jpn*, 1993, **30**, 790–804.
16. M. A. VENKATASWAMY, J. A. SCHNEIDER, J. R. GROZA, A. K. MUKHERJEE, K. YAMAZAKI and K. SHODA: *J. Mater. Sci. Eng. A*, 1996, **207**, 153–158.